

COMMISSIONING AND OPERATION OF THE ARIEL ELECTRON LINAC AT TRIUMF*†

M. Marchetto, F. Ames, Z. Ang, R.A. Baartman, I. Bylinskii, Y.C. Chao, D. Dale, K. Fong, R. Iranmanesh, F. Jones, D. Kaltchev, J. Kavarskas, P. Kolb, S.R. Koscielniak, A. Koveshnikov, M. Laverty, R.E. Laxdal, Y. Ma, L. Merminga, N. Muller, R. Nagimov, R. Nussbaumer, T. Planche, M. Rowe, S. Saminathan, V.A. Verzilov, Z. Yao, Q. Zheng, V. Zvyagintsev
TRIUMF, Vancouver, Canada

Abstract

ARIEL is the new TRIUMF facility for production of radioactive ion beams that will enable the delivery of three simultaneous RIB beams to the ISAC experimental stations. Two additional target stations will produce beams by using either a 50 kW proton or from 500 kW electrons via photo-fission. The electron beam driver is going to be a 50 MeV 10 mA CW superconducting electron linac. The first stage of the e-linac installation is completed and commissioning is underway. The paper will present the e-linac design characteristics, installation, commissioning strategy and current results.

INTRODUCTION

The ISAC (Isotope Separation and ACceleration) facility at TRIUMF produces rare isotope beams (RIB) using the ISOL (Isotope Separation On Lina) method. ISAC uses the TRIUMF cyclotron as driver to accelerate protons at 500 MeV up to 100 μA of current. This is presently the highest power (up to 50 kW of beam power) driver beam for an ISOL facility. It allows to produce the most intense RIB of certain species like ^{11}Li for which yield of $2.2 \cdot 10^4 \text{ s}^{-1}$ has been achieved. The current limitation of ISAC is that only a single RIB is available for fifteen experimental stations distributed in three areas: low, medium and high energy [1].

The ARIEL project [2] is meant to triple the RIB availability by delivering three simultaneous beams. The project consists of augmenting the present proton driver beam from the cyclotron and associated ISAC target stations with the addition of a new electron linac (e-linac) driver and a second proton beam driver from the cyclotron and associated two new target stations and low energy RIB delivery systems as illustrated in Fig. 1. The new e-linac is going to deliver 50 MeV electrons up to 10 mA for a maximum beam power on target of 0.5 MW.

A first stage of the ARIEL installation including a 30 MeV portion of the e-Linac and electron beamlines plus new ARIEL building and infrastructure is now nearing completion. The second phase encompassing the upgrade of the e-Linac to full energy, new target stations new proton beam line and low energy RIB beam lines is now under fund request adjudication.

* Funded under a contribution agreement with NRC (National Research Council Canada)

† Capital funding from CFI (Canada Foundation for Innovation)

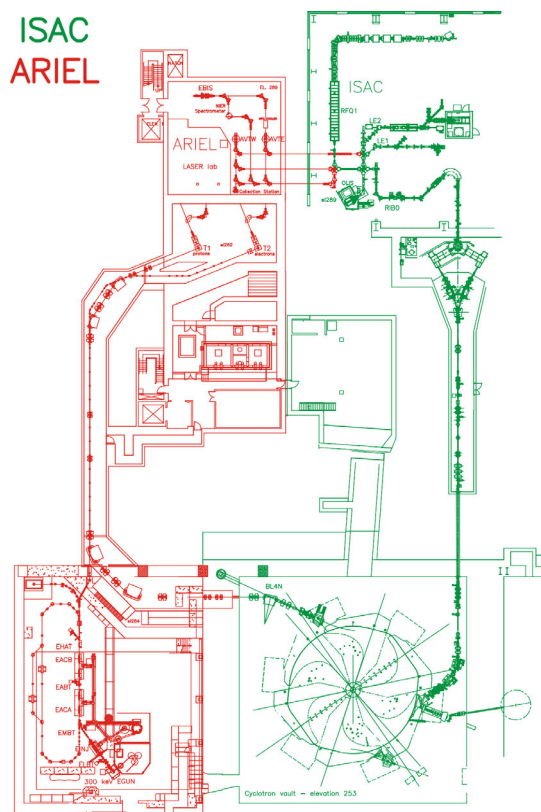


Figure 1: ISAC (green) and ARIEL (red) facilities at TRIUMF.

Accelerated electrons can be used to generate RIBs via the photo-fission process [3]. The electrons are slowed either in the target material itself or in an upstream converter material to generate bremsstrahlung radiation that produce fissions in the actinide target material. The fission production resonance is centered near an incident photon energy of 15 MeV such that the production yield saturates around an electron energy of 50 MeV. Figure 2 shows yield production comparing 10 μA , 500 MeV protons on a 25 g/cm² UCx target and 10 mA, 50 MeV electrons on a Hg converter and 15 g/cm² UCx target. The two production methods are complementary. Electrons produce more neutron rich isotopes with less isobaric contamination. A beam current of 10 mA at 50 MeV is required to produce the goal rates of 10¹³ fissions/sec in an actinide target of sufficient density. This sets the operating boundary envelope for the completed electron linac. The electron linac is housed in a pre-existing shielded former

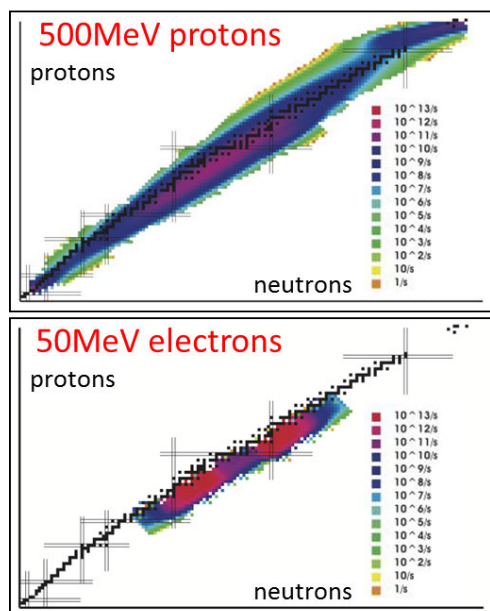


Figure 2: Yield production comparison between $10\ \mu\text{A}$, 500 MeV protons on a $25\ \text{g}/\text{cm}^2$ UCx target (top) and 10 mA, 50 MeV electrons on a Hg converter and $15\ \text{g}/\text{cm}^2$ UCx target (bottom).

experimental hall adjacent to the TRIUMF cyclotron that has been re-purposed as the e-linac accelerator vault (e-hall). The e-linac installation is staged.

E-LINAC DESIGN

The e-hall sits on the west side of the cyclotron vault. Here the stray magnetic field of the cyclotron measures an average of 3 G. The configuration of the e-linac inside the e-hall is shown in fig. 3. The e-linac (depicted in red) is positioned such that a recirculating ring can be accommodated in the future. The ring is part of a future energy recovery linac (ERL) with injection and extraction between 5 – 10 MeV and so a single cavity off-line injector cryomodule (EINJ in fig. 3) was chosen plus two 2-cavity accelerating modules (EACA and EACB).

The e-linac operate at 1.3 GHz. This choice take advantage of the development already made on this technology worldwide. The linac architecture was determined by the choice of final cw beam power and the available commercial cw rf couplers at the design rf frequency of 1.3 GHz. The CPI produced coupler developed with Cornell for the ERL injector cryomodule is capable of operation at 50 kW cw. The cavity design allows two CPI couplers per cavity arranged symmetrically around one end delivering a total of 100 kW of beam loaded power. This sets a maximum gradient per cavity at 10 MV/m. A total of five cavities are required to reach 50 MeV and 0.5 MW beam power.

Electron Gun

The electron source [4] (e-gun) provides electron bunches with charge up to $15.4\ \text{pC}$ at a repetition frequency of

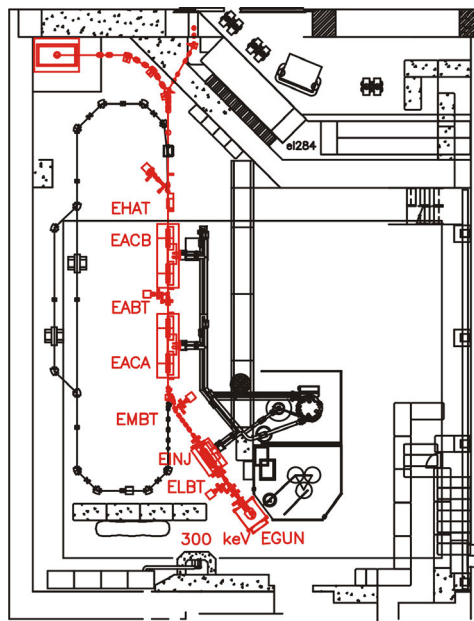


Figure 3: Layout of the ARIEL electron linac.

650 MHz. The main components of the source are a gridded dispenser cathode in a SF6 filled vessel, and an in-air high voltage power supply. The beam is bunched by superimposing a RF modulation to overcome a DC suppression voltage on the grid. Unique features of the gun are its cathode/anode geometry to reduce field emission and transmission of RF modulation via a dielectric (ceramic) waveguide through the SF6. The latter obviates the need for a HV platform inside the vessel to carry the RF generator and results in a significantly smaller/simpler vessel. An impedance network inside an HV shroud matches the waveguide to the cathode.

Cavities

The cavities installed in both the injector and accelerating cryomodules are superconducting nine-cell TESLA type with modified end groups.

Cavity parameters include: $\nu = 1.3\ \text{GHz}$, $L = 1.038\ \text{m}$, $R/Q = 1000$, $E_a = 10\ \text{MV}/\text{m}$. For $Q_0 = 1 \cdot 10^{10}$ the cavity power is $P_{cav} = 10\ \text{W}$.

The end groups are modified to accept the two power couplers and to help push high order modes (HOMs) to dampers located on each end as represented in fig. 4.

On the power coupler end there is a stainless steel (SS) damping tube coaxial with the beam tube and extending

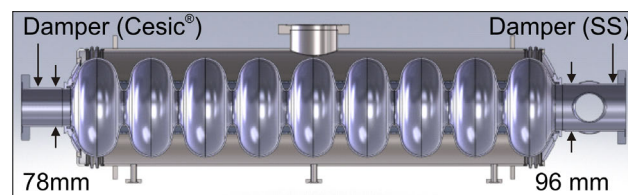


Figure 4: e-linac jacketed cavity with HOM dumper on each end.

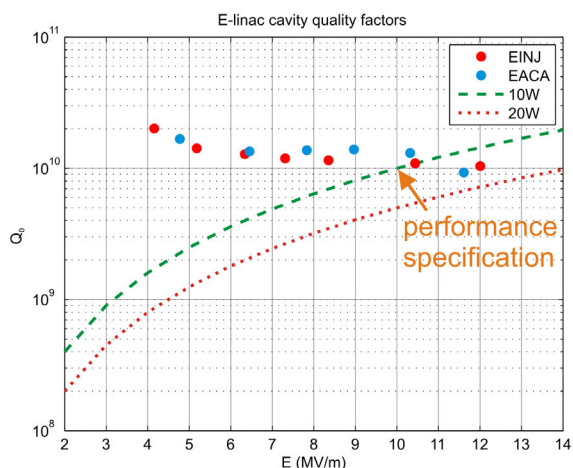


Figure 5: Quality factors for the e-linac installed cavities; both cavities meet specifications.

into the beam tube by 17 mm. On the opposite end of the cavity a coaxial CESIC[®] tube is used [5]. Each tube is thermally anchored at 77 K and thermally isolated from the cavity by a thin walled stainless steel bellows. The dampers are sufficient to reduce the HOMs to meet the beam break-up (BBU) criterion of $R_d/Q \cdot Q_L < 1 \cdot 10^6$. The beam tube diameters on the coupler end and opposite end are 96 mm and 78 mm respectively. The vacuum jacket is made from titanium with a bellows on either end. A single 90 mm diameter chimney allows for large cw rf loads of up to 60 W per cavity assuming a conservative heat transfer of 1 W/cm².

The e-linac cavities are fabricated by PAVAC. The two installed cavities (one in the EINJ, the other in the EACA) meet the specification as represented in fig. 5. The EINJ cavity preparation sequence includes: 120 μm buffer chemical polish (BCP), 800 °C for four hours degas at Fermi National Accelerator Laboratory (FNAL) and 20 μm BCP. The EACA cavity preparation sequence includes: 120 μm buffer chemical polish (BCP), 800 °C for four hours degas and 120 °C bake at Fermi National Accelerator Laboratory (FNAL), high pressure (HP) rinse and 20 μm BCP. A third cavity is under testing for later installation in the EACA [6].

Cryomodules

The cryomodule design is based on the ISAC-II superconducting linac [7]. The module [8] is a top-loading box-like structure with a stainless steel vacuum chamber (see Fig 6).

The cold mass is suspended from the lid and includes a stainless steel strongback, a 2 K phase separator pipe, cavity support posts and the cavity hermetic unit. The hermetic unit consists of the niobium cavities, the end assemblies, an inter-cavity transition (ICT) with a stainless steel HOM damper, the power couplers (FPC) and an rf pick-up. The end assemblies include the warm-cold transition (WCT), CESIC[®] HOM damping tubes and beam-line isolation valves. Other features include a scissor jack tuner and warm motor, liquid nitrogen (LN2) cooled thermal isolation box and two

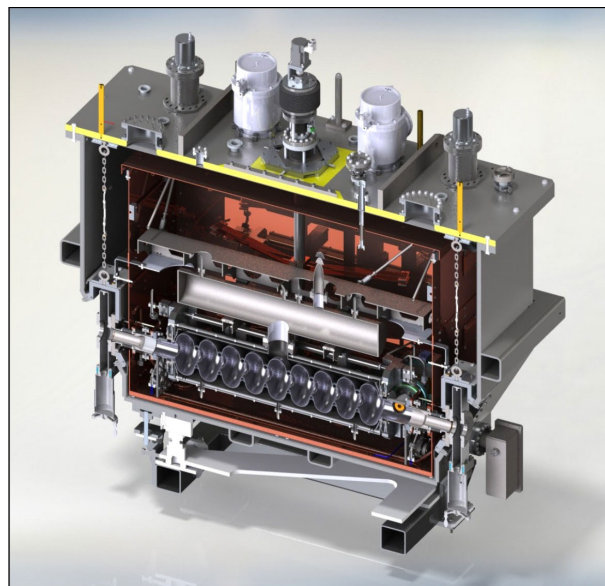


Figure 6: e-linac injector cryomodule rendering cross section.

layers of mu metal and alignment monitoring via a wire position monitor (WPM) diagnostic system. Each cryomodule is outfitted with an on-board 4 K to 2 K cryogenics insert. The insert consists of a 4 K phase separator, a 2.5 gm/sec heat exchanger and a JT expansion valve, a 4 K cooldown valve and a 4 K thermal intercept siphon supply and return. During cooldown the 4 K valve is used to direct liquid helium (LHe) to the bottom of the cold mass until 4 K level is reached. The level in the 4 K reservoir is regulated by the LHe supply valve, the level in the 2 K phase separator is regulated by the JT valve and the 2 K pressure is regulated by the sub-atmospheric line valve. Piping within the module delivers the siphon supply to a number of 4 K thermal intercept points (WCT, ICT and FPC) and then returns the two phase LHe back to the top of the 4 K phase separator.

The cryomodules are first assembled to test the fitting of all the mechanical parts. This mock-up allows also for optimization of the final assembly procedure. The assembly of the hermetic unit composed of cavities, HOM, power couplers, pick-ups and isolation valves, takes place in a class-10 clean room.

Due to unavailability of the third production cavity, the EACA is presently equipped with a single nine-cells cavity and a “dummy” cavity equipped with DC heaters that mimics the cryogenic load in lieu of the second cavity [6].

Cryogenic System

The design of the cryomodules allows a simplified cryogenics system [9]. A standard commercial 4 K cold box is employed delivering 4 K liquid to a supply dewar near atmosphere. The LHe in the dewar is pushed through the cold distribution with slight overpressure (1.3 Bar) and delivered to the cryomodule 4 K reservoir with parallel feed from a common distribution trunk and cold return back from each cryomodule to the exhaust side of the trunk. The distribution

Content from this work may be used under the terms of the CC BY 3.0 licence (© 2015). Any distribution of this work must maintain attribution to the author(s), title of the work, publisher, and DOI.

has a “keep cold” return pipe that joins the supply side of the trunk to the return side. Each cryomodule has an associated variable LHe supply valve. The 4 K supply and return operates as a refrigerator load. The sub-atmospheric system is independent from the cold box and operates as a liquefaction load. Each cryomodule is pumped in parallel from a common pump line while a variable valve controls the pressure. A common pump line leads between the cryomodules and the sub-atmospheric pumps in a separate building. A common valve near the sub-atmospheric pumps optimizes the operating pressure at the pumps for a given mass-flow. The return 2 K exhaust is warmed passively in a counter flow heat exchanger by thermal exchange with the helium high pressure stream going to the cold box.

High Power RF System

The rf system includes one high power rf source for each cryomodule. In Phase I each cryomodule will be driven by a dedicated 300 kW 1.3 GHz klystron. For Phase II one 300 kW klystron will drive EACB while the EINJ will be driven by a 150 kW power source to be determined. The EACA rf power feed is split to feed each of the cavities equally. A further splitting is required to feed each of the power couplers while phase shifters in each leg are used to achieve the proper phase conditions. One LLRF system is used for each cryomodule with a vector sum compensation of voltage and phase drifts in the EACA.

COMMISSIONING

In order to meet a funding dead-line the commissioning (night shifts) was interleaved with installation (day shifts). Individual systems are commissioned first without beam. This allows to check the equipment installation and readiness to transport beam. The electron gun and low energy transport line (ELBT) of the installed hardware in the e-hall were tested with beam in the ISAC-II accelerator vault prior to the e-hall installation.

Electron Gun

The system is installed and conditioned to 320 kV with beam extracted at 300 kV up to the full cw intensity of 10 mA. RF modulation of the grid voltage is demonstrated over a wide duty factor range from 0.01% to cw.

The transverse emittance of the beam as measured with an Allison emittance scanner [10] for a peak current of 10 mA and 1% duty factor is $\epsilon_{rms,norm} = 7.5 \mu\text{m}$ [11]. The transverse emittance is also estimated via tomography reconstruction of transverse profiles as a function of solenoid strength. The result of the reconstruction is represented in fig. 7. The horizontal transverse emittance is effected (split) by the relative low temperature of the gun cathode that results in a non-uniform emission as shown in fig. 8. The low temperature is necessary to produce low intensity beam since the scans are take with a YAG screen. The estimated rms emittances, $5 \mu\text{m}$ for the horizontal and

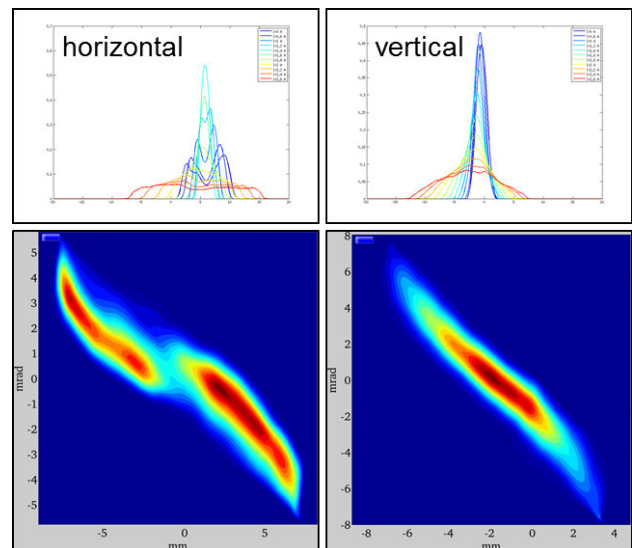


Figure 7: Beam profile as a function of solenoid strength (top) and relative tomography reconstructed transverse emittance (bottom).

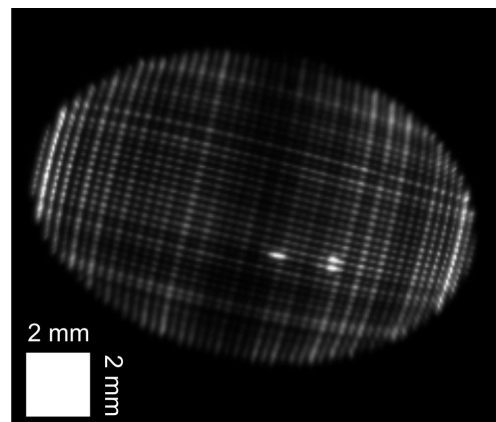


Figure 8: Beam spot image of the cathode at low temperature: the grid structure is visible grid.

$3 \mu\text{m}$ for the vertical, are compatible with the previous measurements [4].

The bunch length as measured with an rf deflecting cavity in the ELBT analyzing leg at a peak current of 1.75 mA and a grid bias voltage of $U_b = -160 \text{ V}$ is ± 12.3 degree with an energy spread of $\Delta E = \pm 500 \text{ eV}$. Estimates based on the measured transconductance ($g_{21} = 23 \text{ mA/V}$) result in a pulse length of $\phi = \pm 10$ degree [4].

Beam Transport Lines

There are three beam transport line sections: low energy (ELBT), medium (EMBT) and high (EHBT). They are respectively the beam lines between the e-gun and the EINJ with beam energy is 300 keV, between the EINJ and the EACA with a beam energy of 10 MeV and downstream of the EACA with beam energy up to 50 MeV.

The ELBT section contains solenoids to provide transverse matching and transportation and orbit correctors.

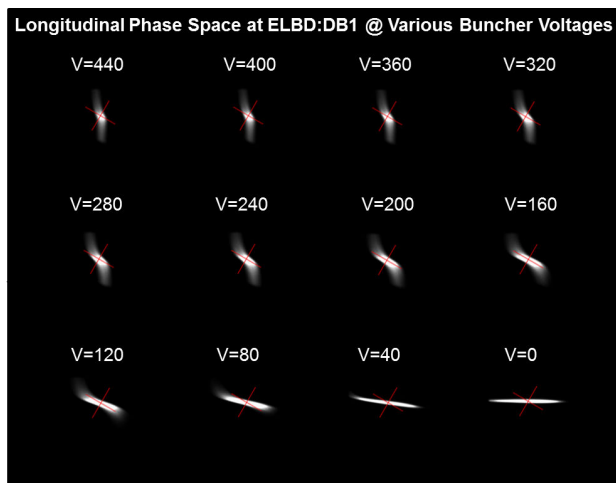


Figure 9: Longitudinal phase space rotation using the TM110 mode rf deflector cavity

Transverse optics measurements showed steering effects and beam spot asymmetry when the first solenoid field was varied. The solenoid design included two split field clamps concentric to the solenoid attached only to the beam pipe for ease of installation. It was discovered that a misalignment of half of the upstream clamp produced an asymmetry in the field. A new design of the clamp is now in place where the clamp is attached only to the solenoid to avoid relative movements.

A 1.3 GHz room temperature ELBT buncher provides longitudinal matching to the EINJ. An analyzing leg branching out of ELBT includes a 90 degree bending spectrometer, diagnostic boxes and a 1.3 GHz TM110 mode rf deflector for bunch length measurements [11]. Figure 9 shows the longitudinal phase space rotation as a function of the buncher voltage as measured downstream of the rf deflector.

The EMBT and EGBT beam lines have quadrupoles for transverse focusing and orbit correctors. Each of these two lines has an analyzing leg to measure the beam energy using a magnetic dipole.

Standard diagnostic in all the beam lines include Faraday cups (FC), profile monitors (YAG and OTR screen), fast wire scanner and non intercepting beam position monitor (BPM).

The beam optic elements use calculated values for the solenoid and quadrupole settings based on beam envelope calculations and magnetic field measurements. Each magnet is characterized by a BH curve measured at TRIUMF.

Helmholtz-like coils surround the beam lines to compensate the cyclotron stray magnetic field. The residual magnetic field on axis can be reduced from 3 G to an acceptable level of < 1 G.

Cryogenics

The ARIEL cryogenic system includes an ALAT LL Cold Box and KAESER FSD571SFC main compressor with a mass flow rating of 112 g/s. In order to arrive at a specifica-

tion the estimated static loads from the distribution and the cryomodules were multiplied by 1.5 while the active load was doubled assuming that either the Q_0 would be lower by a factor of two or the gradient would be increased to 14 MV/m in some modes. This resulted in a mixed mode set point with a refrigeration load of 128 W and a liquefaction load of 220 l/hr (7.6 g/s). Considering these requirements a specification of a pure refrigeration performance of 600 W and a pure liquefaction performance of 280 l/h was defined. The final commissioning produced a pure refrigeration performance of 837 W and a pure liquefaction performance of 367 l/h comfortably above the criteria. Four Busch Combi DS3010-He sub-atmospheric pumping units rated at 1.4 g/s each are installed. More can be added as the 2 K production increases in Phase II.

Cryomodules

One of the main goal of commissioning is to prove acceleration with the installed cryomodules.

The electron beam energy reached downstream of the EINJ is 12 MeV. An early acceleration attempt produced an output energy of just 5.5 MeV [6]. The limitation was due to field emission from the installed cavity that limited the gradient to about 5 MV/m. It was discovered that the SS HOM damper scraped the niobium rf surface during assembly creating particulate. The EINJ cavity was removed, re-etched and re-installed following a different procedure.

The EINJ and EACA cryomodules in the present configuration produce a final energy of 23 MeV. This final energy actually exceeds specification since it is obtained with two cavities one per module.

CONCLUSION

Early stage of commissioning demonstrates that the e-linac equipment meets performance goals. The e-gun is performing reliably and providing the beam quality expected. The installed cavities meet performance specifications and the cryomodules exhibit robust engineering also within specification. The beam optics shows good agreement with simulation even though it still needs to be fully characterized in order to increase the beam power. The e-linac is a tremendous success delivered on a challenging schedule.

REFERENCES

- [1] M. Marchetto, "Commissioning of the 20 MV Superconducting Linac Upgrade at TRIUMF", FROBN0, PAC 2011, New York, USA (2011).
- [2] L. Merminga et al., "ARIEL: TRIUMF's RareIsotopE Laboratory", WEOBA001, IPAC 2011, San Sebastian, SPAIN (2011).
- [3] W.T. Diamond, "A radioactive beam facility using photofission", NIM-A 432 (1999) pp 471-482.
- [4] F. Ames et al., "The TRIUMF ARIEL RF Modulated Thermionic Electron Source", WECF1133, EIC2014, Newport News, Virginia, USA (2014).

- [5] P. Kolb et al., “Cold Tests of HOM Absorber Material for the ARIEL eLINAC at TRIUMF”, NIM-A 734 (2014) pp 60-64, <http://dx.doi.org/10.1016/j.nima.2013.05.031>
- [6] R.E. Laxdal et al., “Status of Superconducting Electron Linac Driver for Rare Ion Beam Production at TRIUMF”, MOIOC01, LINAC2014, Geneva, Switzerland (2014).
- [7] G. Stanford et al. “Engineering and Cryogenic Testing of the ISAC-II Medium Beta Cryomodule”, THP16, LINAC 2004, Lübeck, Germany.
- [8] R.E. Laxdal et al., “The Injector Cryomodule for the ARIEL e-Linac at TRIUMF”, MOPB091, LINAC2012, Tel-Aviv, Israel (2012).
- [9] I. Bylinskii et al., “Particularities of the ARIEL e-Linac Cryogenic System”, WEPMA005, this conference proceedings.
- [10] A. Laxdal et al., “Allison Scanner Emittance Diagnostic Development at TRIUMF”, THIOC02, LINAC2014, Geneva, Switzerland (2014).
- [11] R.E. Laxdal et al., “TRIUMF/VECC e-Linac Injector Beam test”, MOPB026, LINAC2012, Tel-Aviv, Israel (2012).